Azamacrocyclic complexes of Group VIII metals as catalysts for oxygen electroreduction in alkaline solutions

A. Yu. Tsivadze,[a] M. R. Tarasevich,[a] E. A. Maleeva,[a] V. E. Baulin,[a,b] and I. P. Kalashnikova[a,b]*

[a]*A. N. Frumkin Institute of Physical Chemistry and Electrochemistry, Russian Academy of Sciences, Building 4, 31 Leninsky prosp., 119991 Moscow, Russian Federation. Fax: +7 (495) 952 5308. E-mail: e_maleeva@mail.ru*
[b]*Institute of Physiologically Active Compounds, Russian Academy of Sciences, 1 Severnyi pr-d, 142432 Chernogolovka, Moscow Region, Russian Federation*

The kinetics of catalytic electroreduction of oxygen in a 1 *N* KOH solution was studied by the rotating disk electrode (RDE) method. Azamacrocyclic iron and ruthenium complexes of the porphyrin and phtalocyanine series were used as catalysts. The reduction of oxygen was also studied on both the individual complexes and the same complexes supported on carbon supports (XC72R and graphene). The catalytic activity and selectivity of the complex is determined, to a high extent, by the nature and electron-donor properties of the metal atom in the complex and, to a lesser extent, by the structure of the organic ligand.

Key words: electroreduction of oxygen, catalysts, phtalocyanine and porphyrin complexes, iron, ruthenium.

Among the works on macrocyclic metal complexes as catalysts in the electroreduction of oxygen two directions can be recognized. The demand and high cost of the catalysts based on the Platinum group metals stimulated the search for alternative systems. These include macrocyclic metal complexes, first of all, those of the porphyrin and phthalocyanine series.[1] The purpose of these works was the preparation of catalysts efficient in oxygen reduction. In addition, the mechanism of electrocatalysis on the macrocyclic complexes was studied in terms of the concepts of molecular catalysis,[2] which made it possible to extend the understanding of processes and regularities of electrocatalysis on such complicated organometallic systems. Large experimental material on the catalytic electroreduction of oxygen on the macrocyclic metal-containing complexes has been accumulated within the last two decades. However, the route of the reaction, its step character and mechanism, and the nature of the active site responsible for adsorption of molecular oxygen have not yet been elucidated. There are conflicting, often opposite, estimates of the activity and selectivity of molecular complexes with respect to oxygen reduction. For the most part, studies were carried out under model conditions, which involve monolayer or near monolayer fillings of the surface of the smooth electrode with the adsorbed complex. The purpose of the present work is to compare the activity and selectivity of the macrocyclic complexes of metals in various oxidation states both under model conditions on the smooth electrode and under conditions relevant to complicated catalytic systems supported on carbon supports.

Graphene-like materials were used as supports because of high conductivity and chemical stability of graphene and graphene-like materials (Gre) can be used in future for preparation of supported catalysts.[3] The proofs obtained recently for the intrinsic catalytic activity of graphene[4] confirm that the study of graphene-like materials as catalysts is promising.

Experimental

Carbon materials. The graphene-like material was synthesized from graphite (Alfa Aesar, A Johnson Matthey Company, 99.9995%) using an earlier published procedure.[5] According to the results of the complex physicochemical study, the obtained material contains ~80 at.% of carbon and up to 20 at.% of oxygen. Based on the data of atomic force microscopy, the material represents associates of fragments of the initial graphite with the thickness of five monolayers. The average specific surface determined by the electrochemical method is ~400 $m^2 g^{-1}$. Turbostrate carbon XC72R (Cabot Corp., specific surface ~220 $m^2 g^{-1}$, oxygen content 6 at.%) was used as received.

Individual non-supported complexes. The complexes of iron(II) hexadecachlorophthalocyanine (Fe^{II} HDC PC) and iron(III) tetraphenylporphyrin (Fe TPP) (Sigma—Aldrich) were used as received. The complexes of iron phthalocyanine (Fe^{II-III} PC) and ruthenium (Ru^{IV} PC) were synthesized at the Laboratory of Novel Physicochemical Problems of the A. N. Frumkin Institute of Physical Chemistry and Electrochemistry (Russian Academy of Sciences) using the methods similar to the

Published in Russian in *Izvestiya Akademii Nauk. Seriya Khimicheskaya,* No. 10, pp. 2386—2392, October, 2015.
1066-5285/15/6410-2386

known procedures.[6] The synthesized compounds were purified by consecutive washing with hot solvents (hexane, acetone, and methanol) using the Soxhlet apparatus followed by reprecipitation with water from concentrated sulfuric acid. The synthesized complexes were characterized by IR, UV, and ESR spectra confirming the structure of the complex and the oxidation state of the central atom.

A solution of the complex in a low-boiling solvent was prepared to obtain a thin layer of the complex on the glassy carbon (GC) electrode. A weighed sample of the complex in the solvent was treated if necessary with ultrasound for 10—60 min until a complete dissolution. The solution was deposited on the electrode surface and dried at ~20 °C, and then a droplet of a 5% solution of Nafion (Nafion®, Aldrich) in ethanol was deposited. Nafion is a sulfated fluorovinyl copolymer of perfluoroethylene, polymeric electrolyte with ionic conductivity of the polymer type that anchors a finely dispersed complex on the GC electrode surface. Then the supported complex was dried for 30 min in air. The calculated amount of the complex on the GC electrode surface was 7—70 monolayers.

Macrocyclic complexes supported on carbon carriers. A weighed sample of a carbon carrier was dispersed in the corresponding solvent (hexane, acetone, chloroform, DMF, or a mixture of solvents) optimum for the dissolution of this type of the complex. A weighed sample of the complex taken in order to obtain the concentration of the complex equal to 5 wt.% was dissolved with ultrasonication in an appropriate solvent, and then the electronic absorption spectrum was recorded. After this, the solution was added to a dispersion of the carbon material. The obtained mixture was ultrasonicated taking samples for the spectrophotometric control of the content of the complex in a solution. The ultrasonic treatment was repeated for 10—180 min followed by mechanical stirring for 2—10 days. The deposition of the complex was considered complete when no absorption band could be observed (Fig. 1). Then the mixture was washed on a centrifuge with ethanol and dried for 12 h in a drying box at 90 °C. The absorption maximum at 400—500 nm is a characteristic feature of the macrocyclic metal complexes, and the molar absorption coefficient in this range is directly proportional to the concentration of the complex in the solution. The decrease in the maximum intensity upon mixing with a dispersed carbon carrier indicates a decrease in the concentration of the complex in the solution. Thus, the absorbance, for example, near 415 nm for Fe^{III} TPP can serve as a measure of the amount of the complex adsorbed on the carbon support. The complete extraction of the complex from solution is accompanied by the absence of absorption in this range (see Fig. 1, curve *4*). There is an opinion[7] that the appearance of an additional peak at 375 nm after ultrasonication is an indication to the association of the complex and, first of all, the formation of dimers. The prolonged treatment of the mixture with a carbon carrier results in the disappearance of absorption at this wavelength. This suggests that the complex is adsorbed in the form of associates.

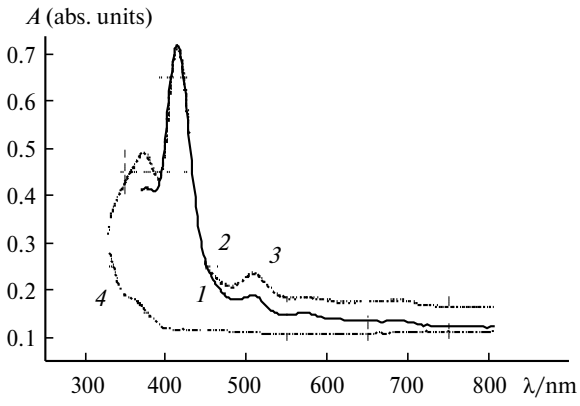

Fig. 1. Spectra of Fe^{III} TPP recorded in acetone at $l = 0.5$ cm: initial Fe^{III} TPP (*1*), Fe^{III} TPP after ultrasonic treatment (40 min) and mixing with graphene (*2*), initial Fe^{III} TPP after ultrasonication (70 min) and mixing with graphene (*3*) and after mixing for 10 days (*4*).

Instrumental measurements. Electrochemical measurements were carried out with an IPC Pro potentiostat (A. N. Frumkin Institute of Physical Chemistry and Electrochemistry, Russian Academy of Sciences) using a system with a rotating disk electrode (NPO Volta, Russia) at the GC electrode (geometric surface area 0.07 cm^2) in a solution of 1.0 *M* KOH. Cyclic voltammetric curves (CV) were recorded either in a solution deoxygenated by argon purging or in a solution saturated with oxygen at 20 °C with a sweep rate of 5, 10, 20, and 50 mV s^{-1}. Polarization curves were obtained with a sweep rate of 5 mV s^{-1} at 60 °C; oxygen was preliminarily passed through the solution for 30 min, and then oxygen was passed above the solution during the whole cycle of measurements. Electronic absorption spectra were recorded on a Specord M-40 spectrophotometer (Carl Zeiss, Jena, Germany).

Results and Discussion

Non-supported individual complexes. The cyclic voltammetric curves of the individual iron and ruthenium complexes supported directly on the GC electrode are presented in Figs 2—6. In an inert atmosphere all cyclic curves are characterized by a high degree of irreversibility caused, possibly, by a low conductivity of the film of the complex on the electrode surface (according to the calculations, the amount of the supported complexes corresponds to a thickness of 7—70 monolayers). It appears that an inert atmosphere non-supported iron(II—III) phthalocyanine and iron(III) TPP are inactive in the indicated potential ranges. Iron(II) HDC PC and ruthenium(IV) PC give conjugated peaks in the cyclic curve. For example, for iron(II) HDC PC, a broad diffuse peak in a range of 0—100 mV corresponds to the anodic peak at 400 mV (peak 1). When the voltammetric curve is presented in the differential form (see Fig. 4), two unpronounced cathodic peaks with potentials of ~100 (peak 2) and ~20 mV (peak 3) can be distinguished in this range. The substantial difference in potentials of the conjugated peaks indicates a significant degree of irreversibility of the corresponding electrochemical reactions. The values of peak potentials depend linearly on the logarithm of the sweep rate at 5—50 mV s^{-1} (Fig. 7).

The theoretical dependence of the peak potential on the potential sweep rate under the conditions of strong adsorption of the oxidized and reduced forms on the electrode surface was derived for the general case.[8] When the electrochemical process is strongly irreversible as indicated by differences in peak potentials $\Delta E_p > 200$ mV[9]

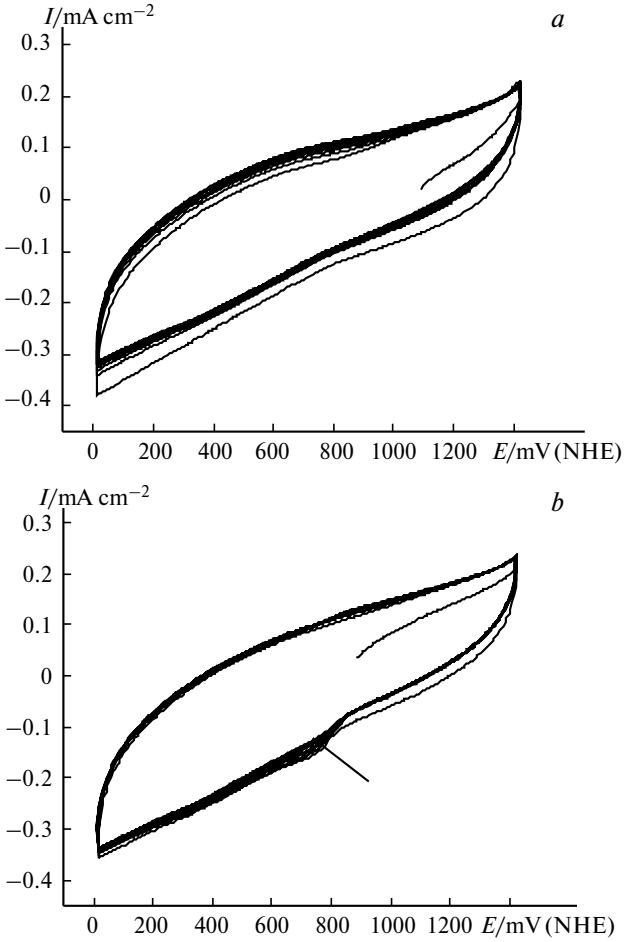

Fig. 2. CV curves for the individual complex Fe^{III} TPP in 1 *M* KOH (20 °C) detected at a sweep rate of 50 mV s^{-1} in argon (*a*) and oxygen (*b*); NHE is normal hydrogen electrode.

taken as a criterion, the equation of the dependence of the cathodic peak potential E_p^c on the sweep rate *S* takes the form

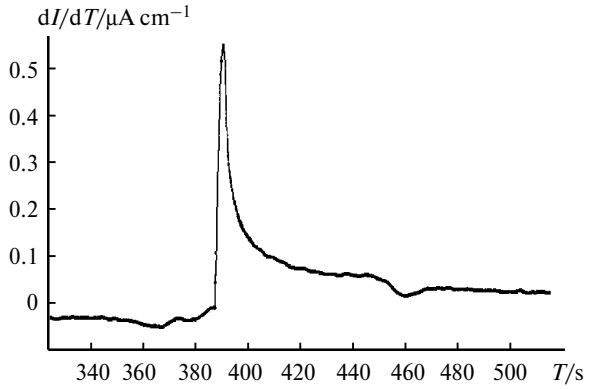

Fig. 4. Fragment of the voltammetric curve as a time derivative dI/dT (sweep rate 5 mV s^{-1}). Local extremes of the derivative correspond to the cathodic peaks at the moments ~375 and 385 s and to the anodic peak at the moment ~460 s.

$$E_p^c = E^j - [RT/(\alpha nF)] \ln(\alpha/m),$$

where E_p^c is the peak potential (V) at the sweep rate *S* (V s^{-1}), E^j is the standard potential (V), *n* is the number of electrons involved in the electrochemical step, α is the transfer coefficient in the electrochemical step, *T* is temperature, *R* is the universal gas constant, and *F* is Faraday´s constant; $m = (RT/F)[k_0/(nS)]$, where k_0 is the rate constant of the electron transfer (s^{-1}). The slope of the $dE_p^c/d(\log S)$ plot of the cathodic peaks is 157 and 102 mV corresponding to $\alpha n \approx 0.4$ and 0.6, respectively. Accepting in the first approximation that $\alpha \approx 0.5$, it can be assumed that each cathodic peak corresponds to the one-electron transfer. As the sweep rate increases, the peaks approach each other and become almost indiscernible. The slope of the plot of the anodic peak potential *vs* potential sweep rate is only 18 mV. Such a low value possibly indicates a substantial degree of reversibility of the anodic process, although the conjugated cathodic process is strongly irreversible. As in the earlier described case,[10] it can be assumed

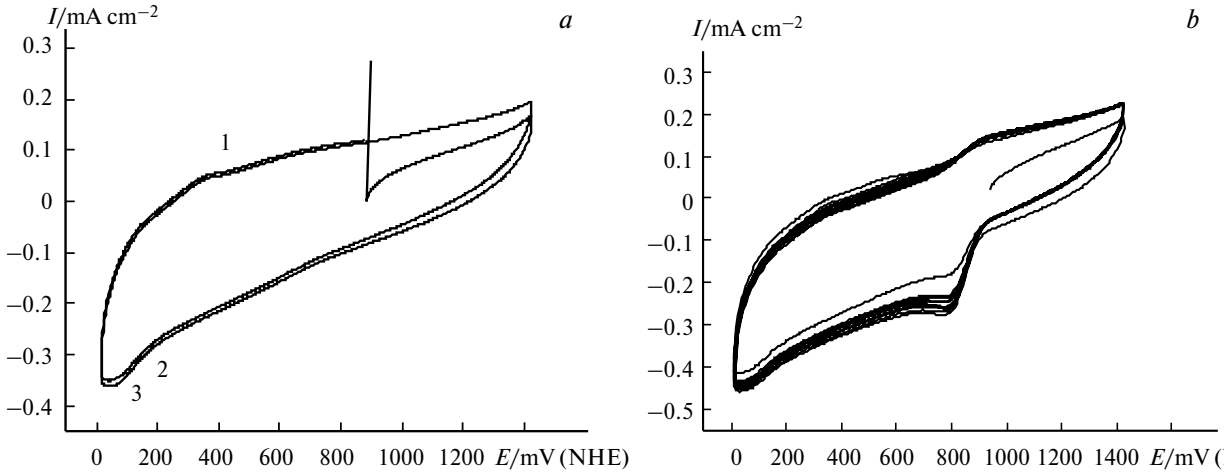

Fig. 3. CV curves for the individual complex Fe^{II} HDC PC in 1 *M* KOH (20 °C) detected at a sweep rate of 50 mV s^{-1} in argon (*a*) and oxygen (*b*).

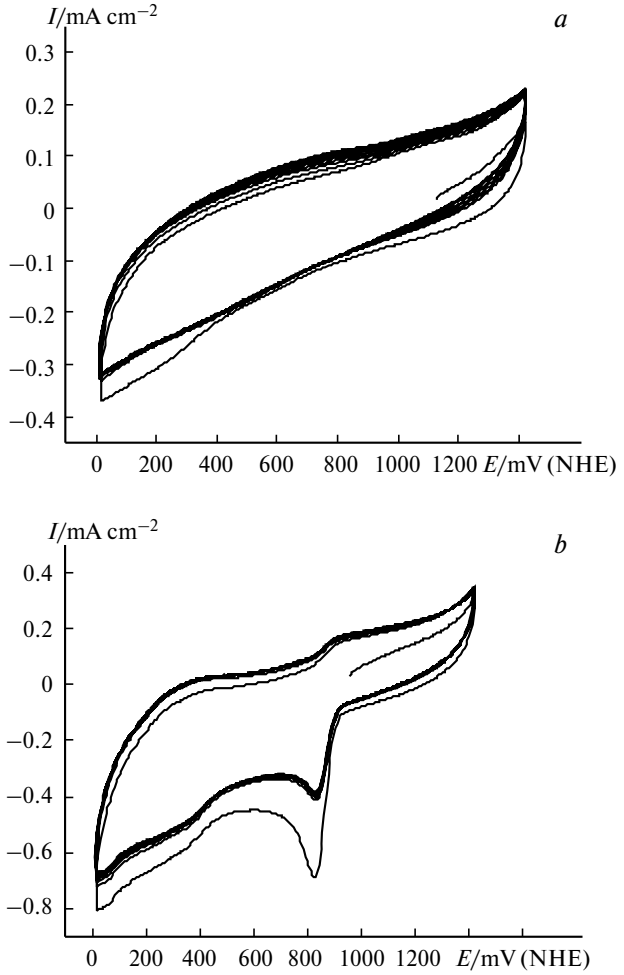

Fig. 5. CV curves for the individual complex Fe^{II-III} PC in 1 *M* KOH (20 °C) detected at a sweep rate of 50 mV s^{-1} in argon (*a*) and oxygen (*b*).

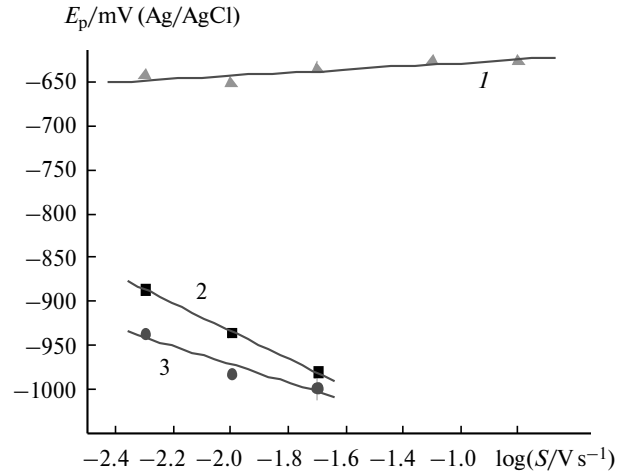

Fig. 7. Potentials of peaks 1—3 for Fe^{II} HDC PC on the GC electrode *vs* sweep rate; 1.0 *M* KOH, 20 °C, argon.

that each cathodic peak corresponds to the addition of an electron to the phthalocyanine ring to form charged complexes.

However, an alternative scheme is also possible that assumes the addition of an electron to the electronic system of the central metal ion.[11] In this case, a similar mechanism can hardly be expected to be operative, since iron in this complex is in a low oxidation state and the standard potential of the Fe^{II}—Fe^{III} transition in the form of the Fe^{II} PC complex is ~0.9 V (NHE) under the given conditions.[12] Two cathodic peaks and the single anodic peak indicate the formation of an identical reduction product from different initial states. These can be phthalocyanine molecules oriented in different ways on the electrode surface (parallel or perpendicular to the surface) or different

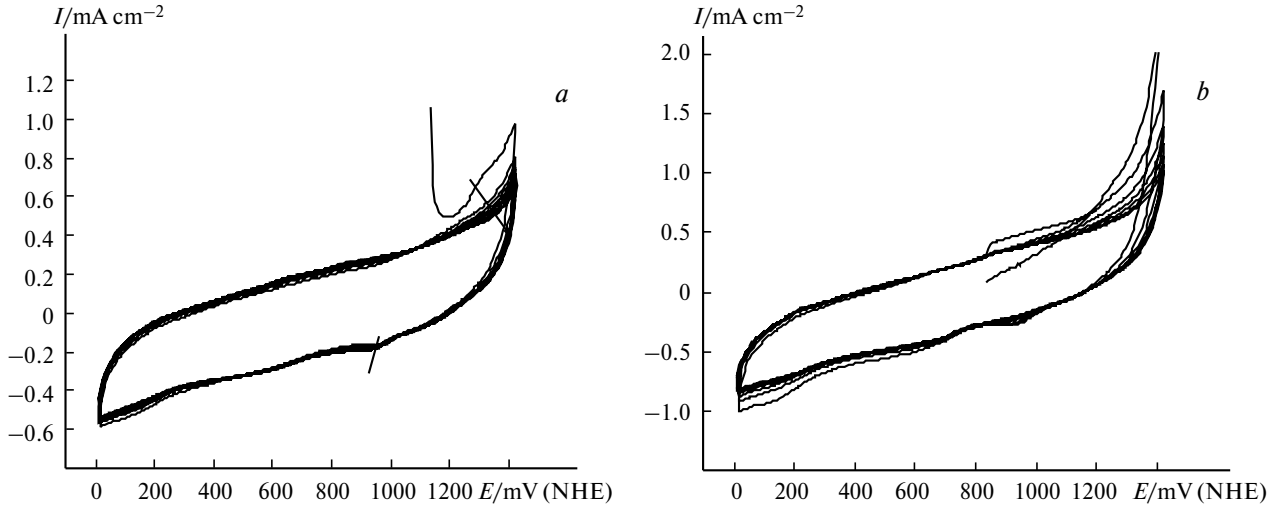

Fig. 6. CV curves for the individual complex Ru^{IV} PC in 1 *M* KOH (20 °C) detected at a sweep rate of 50 mV s^{-1} in argon (*a*) and oxygen (*b*).

polymorphous forms of phthalocyanine (α and β).[13] There is a probability of reduction of the dimeric form of the complex simultaneously with the monomeric form. A possible formation of a dimer is indicated by the presence of an additional peak in the electronic spectrum of the complex in the short-wavelength range (see Fig. 1, *a*) that appeared after ultrasonication.

The studied complexes interact with dissolved oxygen in different ways (see Figs 2, *b*; 3, *b*; 5, *b*; and 6, *b*).

The CV of the complexes containing iron in the low oxidation state in the presence of oxygen exhibit distinct regions of molecular oxygen adsorption—reduction. At the same time, iron(III) TPP and ruthenium(IV) PC adsorb almost no oxygen under the indicated conditions. These data suggest that the complex containing the metal in the low oxidation state (Fe^{II} HDC PC) will be more active in the reduction of oxygen.

In fact, the study of oxygen reduction on individual complexes on a rotating disk electrode in 1.0 *M* KOH shows that the activity in oxygen reduction is directly related to the ability to adsorb oxygen (Fig. 8).

The polarization curve of oxygen reduction on Fe^{III} TPP has two poorly pronounced waves corresponding to the two-step reduction of oxygen. The analysis of the dependence of the inverse current on the inverse rotation rate using the Levich—Koutecky method[8] shows that the first wave corresponds to the two-electron reduction of oxygen to peroxide ion and the second wave corresponds to the further reduction of peroxide to water. The reduction of oxygen on Ru^{IV} PC also proceeds in two steps, and the number of electrons participating in the first step is ~2.

The reduction of oxygen on Fe^{II} HDC PC proceeds in one step, and the number of electrons is $n \approx 3.8$, which is close to a theoretical value of 4; *i.e.*, the complex to a significant extent catalyzes the direct four-electron reduction of oxygen to water. Using the Levich equation value the theoretically calculated value of the limiting diffusion current for the four-electron reaction was found to be 3.75 mA cm^{-2}, which is consistent with the experimental value of limiting current equal to 3.25 mA cm^{-2} for oxygen reduction on Fe^{II} HDC PC. The activity of Fe^{II-III} PC and Ru^{IV} PC is intermediate between those of the complexes of trivalent and divalent iron (Fe TPP and Fe^{II} HDC PC, respectively). The number of electrons involved in the reduction is $n \approx 2.5$—3.1.

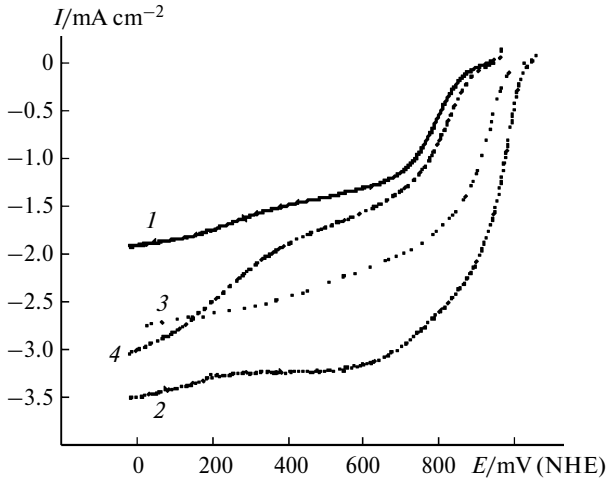

Fig. 8. Polarization curves for oxygen reduction on the individual non-supported complexes at the rotating disk electrode; 1.0 *M* KOH, 60 °C, 1600 rpm: Fe^{III} TPP (*1*), Fe^{II} HDC PC (*2*), Fe^{II-III} PC (*3*), and Ru^{IV} PC (*4*).

The catalytic activity of materials in oxygen reduction can be expressed by the reaction rate or an equivalent value of $\partial E/\partial \log I$, where E is the potential, and I is the current of oxygen reduction. Under the kinetically controlled conditions (*i.e.*, at the current that does not exceed 0.5 of the value of limiting diffusion current), the dependence of E on $\log I$ is linear, and the value of the slope with allowance for the adsorption isotherm of an electroactive particle can indicate the nature of the rate-limiting step. The rate constant of the electrochemical step is proportional to the half-wave potential $E_{1/2}$, and the stationary potential determines the energy of adsorption of the electroactive particle under other equivalent conditions.

The kinetic parameters of oxygen reduction on the individual non-supported complexes are presented in Table 1.

The values of slopes $\partial E/\partial \log I$ can be divided into two rather distinct groups. The first group includes values of 65—75 mV corresponding to a slow step of addition of the first electron to the adsorbed oxygen molecule during oxygen reduction on the macrocyclic complexes in the range of high pH values.[11] The second group contains values of 35—45 mV corresponding[15] to slow step of the second electron addition to the adsorbed and partially ionized oxygen molecule.

The first step of oxygen electroreduction is the adsorption of the oxygen molecule on the macrocyclic complex with a partial charge transfer. Since the ability of the complex to adsorb to oxygen revealed in the CV in the presence of O_2 correlates with the presence of the metal atom in the

Table 1. Kinetic parameters for oxygen reduction on the individual non-supported complexes[a]

Complex	$E_{1/2}$	E^b_{st}	$\partial E/\partial \log I$ /mV decade^{-1}
	mV		
Fe^{III} TPP	802±5	931±5	66
Fe^{II-III} HDC PC	891±5	1040±5	47
Fe^{II-III} PC	951±5	1024±5	35
Ru^{IV} PC	796±5	939±5	79

[a] Conditions: 1.0 *M* KOH, rotating disk electrode 3100 rpm, 60 °C.
[b] Stationary potential.

low or intermediate oxidation state in the macrocycle molecule, it can be assumed that oxygen is adsorbed on the metal. The metal in a high oxidation state (Fe^{III}, Ru^{IV}) has no donating properties and cannot form a charge-transfer complex. This assumption is supported by the observation that Fe^{III} TPP is catalytically nearly inactive. It is most likely that oxygen adsorption on the nitrogen atoms of the macrocyclic complex plays a substantially lower role.

Four variants of the geometric position of the adsorbed oxygen molecule on the central atom of iron-containing phthalocyanine are possible (Fig. 9). As indicated by model calculations, the configuration shown in Figs 9, *c* and *d* are energetically preferable. In this configuration, two oxygen atoms are separated by the same distance from the central metal atom and have the same charge, which makes equally possible the reduction on both atoms and thus enhances the probability of the simultaneous reduction, *i.e.*, four-electron reaction. At the same time, the vertical position of the oxygen molecule on the central atom (see Fig. 9, *a* and *b*) results in the nonuniform charge distribution on two oxygen atoms, which facilitates the stepped reduction, *i.e.*, the occurrence of consecutive two-electron reactions.

Complexes supported on carbon carriers. The polarization curves of oxygen reduction on the iron complexes supported on graphene and XC-72R are presented in Fig. 10.

The mutual arrangement of the curves and the stepped character of the reduction process are similar to those described for the individual complexes. The reduction on Fe^{III} TPP proceeds in two steps, and the stationary potential is 838 mV. The reduction of oxygen on Fe^{II} HDC PC starts at much higher positive potentials (970—990 mV), indicating a substantially stronger adsorption of oxygen on this complex. The curve contains only one wave with a half-wave potential of ~890 mV. The replacement of Gre by XC72R exerts almost no effect on the rate and selectivity of oxygen reduction on Fe^{II} HDC PC. As in the case of the individual non-supported complexes, Fe^{II-III} PC and Ru^{IV} PC are intermediate between the least and most active catalysts.

The kinetic parameters of oxygen reduction on the supported complexes are given in Table 2.

The values of stationary potentials correlate with the ability of the complexes to adsorb oxygen. As for the non-supported complexes, two groups of catalysts can be distinguished with different slopes $\partial E/\partial \log I$, and the presence of the support and its type exerts no effect on the mechanism of oxygen reduction, which is governed, most likely, only by the nature of the complex and central atom.

The selectivity of oxygen reduction on the supported catalysts in the range of the second wave potentials was determined by the analysis of the limiting current dependence on the rotation rate using the Levich—Koutecky method[8] (Table 3).

Thus, the presence and the nature of the carbon support do not affect the selectivity of the complexes in oxygen reduction, which is expressed by the total number of electrons involved in the reaction. Regardless of the presence of the support, the complex having the metal in the lowest oxidation state (Fe^{II} or Ru^{IV}) is most selective. In addition, the replacement of turbostrate carbon XC72R by a graphene-like material did not either result in any effects on the kinetics of oxygen reduction. However, it can be expected that the fragments of graphite ordered layers of graphene (containing up to five graphite mono-

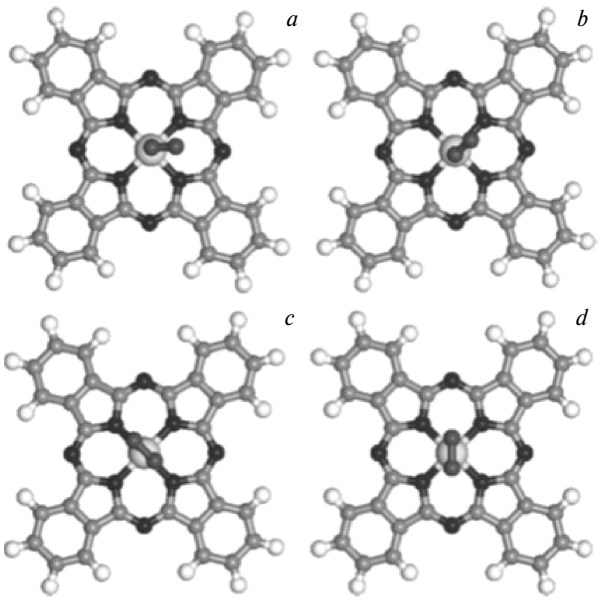

Fig. 9. Optimized structures of the activated iron PC complex with adsorbed molecular oxygen.[16]

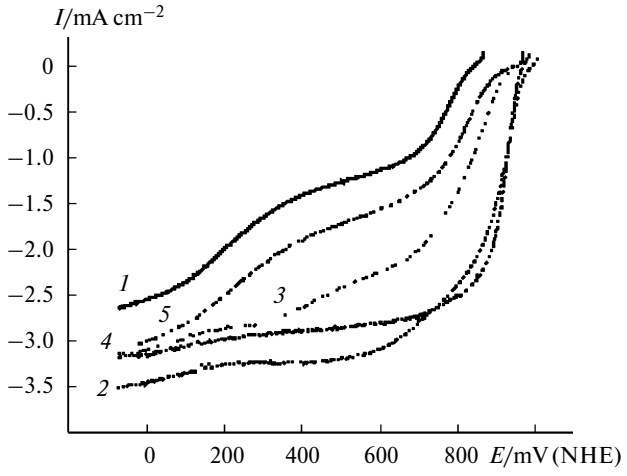

Fig. 10. Polarization curves for oxygen reduction on the complexes supported on the carbon carriers (1.0 *M* KOH, 60 °C, rotating disk electrode 1600 rpm: Fe^{III} TPP on graphene (*1*), Fe^{II} HDC PC on graphene (*2*), Fe^{II-III} PC on graphene (*3*), Fe^{II} HDC PC on XC725R (*4*), and Ru^{IV} PC on graphene (*5*).

Table 2. Kinetic parameters for oxygen reaction on the complexes supported on the carbon carriers*

Complex	$E_{1/2}$	E_{st}	$\partial E/\partial \log I$ /mV decade^{-1}
	mV		
Gre+Fe^{III} TPP	780±5	838±5	59
Gre+Fe^{II} HDC PC	886±5	989±5	42
Gre+Fe^{II} HDC	847±5	942±5	60
XC72R+ Fe^{II} HDC PC	890±5	967±5	44
Gre+Ru^{IV} PC	824±5	942±5	82

* Conditions: 1.0 *M* KOH, rotating disk electrode 3100 rpm, 60 °C.

Table 3. Number of electrons (*n*) involved in the reaction of oxygen reduction on the individual and supported catalysts*

Type of catalyst	*n*
Individual	
Fe^{II-III} HDC PC	3.8
Fe^{III} TPP	1.8
Fe^{II-III} PC	3.1
Ru^{IV} PC	2.5
Supported	
Gre + Fe^{II} HDC PC	3.4
XC72R + Fe^{II} HDC PC	3.4
Gre + Fe^{III} TPP	1.7
Gre + Fe^{II-III} PC	2.6
Gre + Ru^{IV} PC	2.4

* Conditions: 1.0 *M* KOH, rotating disk electrode, 60 °C.

layers[5]) would interact with adsorbed planar molecules of the complexes more strongly that turbostrate carbon, and this would lead to a higher stability of the formed associates.

To conclude, the mechanism of oxygen electroreduction on the azamacrocyclic complexes of the Group VIII metals is governed, to a significant extent, by the nature and electron-donor properties of the central metal atom. The macrocomplexes having the metal atom in the lowest oxidation state are most active and selective as catalysts. For example, Fe^{II} HDC PC ensures an almost four-electron reduction of oxygen to water under the studied conditions. However, this conclusion based on the calculations using the Levich—Koutecky equation is formal to a considerable extent. The used procedure does not allow one to distinguish the one-step reaction of oxygen reduction with the O—O bond cleavage and the consecutive reduction in two two-electron steps.[14] Experiments on a rotating ring-disk electrode are needed to reveal the true route of oxygen reduction on these complexes.

This work was financially supported by the Russian Foundation for Basic Research (Project No. 13-03-00317).

References

1. J. H. Zagal, M. A. Paez, J. F. Silva, in *N^4-Macrocyclic Metal Complexes*, Eds J. H. Zagal, F. Bedioui, J.-P. Dodelet, Springer, New York, 2006.
2. J. Masaa, K. Ozoemenab, W. Schuhmanna, J. H. Zagal, *J. Porphyrins Phthalocyanines*, 2012, **16**, 761.
3. M. R. Tarasevich, V. A. Bogdanovskaya, O. A. Lozovaya, E. A. Maleeva, E. M. Kol´tsova, *Al´ternativnaya energetika i ekologiya* [*Alternative Power Engineering and Ecology*], 2012, **1**, 82 (in Russian).
4. M. S. Ahmed, S. Jeon, *J. Power Sources*, 2012, **218**, 168.
5. E. A. Maleeva, M. R. Tarasevich, *Russ. J. Phys. Chem. A* (*Engl. Transl.*), 2014, **88**, 1396 [*Zh. Fiz. Khim.*, 2014, **88**, 1216].
6. S. I. Mikhalenko, V. M. Derkacheva, E. A. Luk´yanets, *Zh. Org. Khim.*, 1981, **51**, 1650 [*J. Org. Chem. USSR* (*Engl. Transl.*), 1981, **51**, No. 7].
7. G. P. Gurinovich, A. N. Sevchenko, K. N. Solov´ev, *Usp. Fiz. Nauk* [*Advance in Physical Science*], 1963, **79**, No. 2, 2 (in Russian).
8. A. J. Bard, L. Faulkner, *Electrochemical Methods, Fundamentals, and Applications*, John Wiley and Sons, New York, 1981, 236; 594.
9. E. Laviron, *J. Electroanal. Chem.*, 1979, **101**, 19.
10. A. R. Ozkaya, E. Hamuryudan, Z. A. Bayir, O. Bekaroglu, *J. Porphyrins Phthalocyanines*, 2000, **4**, 689.
11. M. R. Tarasevich, K. A. Radyushkina, V. A. Bogdanovskaya, *Elektrokhimiya porfirinov* [*Electrochemistry of Porphyrins*], Nauka, Moscow, 1991, 312 pp. (in Russian).
12. G. I. Cardenas-Jiron, M. A. Gulppi, C. A Caro, R. del Rio, M. Paez, J. H. Zagal, *Electrochim. Acta*, 2001, **46**, 3227.
13. F. Iwatsu, *J. Phys. Chem.*, 1988, **92**, 1678.
14. M. R. Tarasevich, E. I. Khrushcheva, V. Yu. Filinovskii, *Vrashchayushchiisya diskovyi elektrod s kol´tsom* [*Rotating Ring-disk Electrode*], Nauka, Moscow, 1987, 247 pp. (in Russian).
15. E. Yeager, in *Intern. Society of Electrochem., 31st Meeting: Extend. Abstr.*, Ed. N. Vecchi, IES, Venice, Vol. **1**, 131.
16. G. Wang, N. Ramesh, A. Hsu, D. Chu, R. Chen, *Mol. Simulation*, 2008, **34**, 1051.

Received September 3, 2014;
in revised form April 20, 2015